

# The Kinetic and Microkinetic Model for Steam Reforming of Methanol under External Electric Field

Changming Ke,<sup>1,2</sup> Zijing Lin,<sup>3</sup> and Shi Liu<sup>1,2,\*</sup>

*<sup>1</sup>Key Laboratory for Quantum Materials of Zhejiang Province,  
School of Science, Westlake University,  
Hangzhou, Zhejiang 310024, China*

*<sup>2</sup>Institute of Natural Sciences, Westlake Institute for Advanced Study,  
Hangzhou, Zhejiang 310024, China*

*<sup>3</sup>Hefei National Laboratory for Physical Sciences at Microscales,  
CAS Key Laboratory of Strongly-Coupled Quantum Matter Physics, Department of Physics,  
University of Science and Technology of China, Hefei 230026, China*

## I. DIPOLE MOMENT AND POLARIZABILITY OF ADSORBATES AND TRANSITION STATES IN SRM

The EEF-induced energy change is,

$$\begin{aligned}\Delta\Delta E_a[\mathbf{F}] &= \Delta E_a[\mathbf{F}] - \Delta E_a^0 = -(\mathbf{d}_{s+\text{TS}^*} - \mathbf{d}_{s+\text{R}^*}) \cdot \mathbf{F} - \frac{1}{2}(\alpha_{s+\text{TS}^*} - \alpha_{s+\text{R}^*})\mathbf{F}^2 \\ \Delta E_{\text{ad}}[\mathbf{F}] &= E_{\text{ad}}[\mathbf{F}] - E_{\text{ad}}^0 = -(\mathbf{d}_{s+i} - \mathbf{d}_s) \cdot \mathbf{F} - \frac{1}{2}(\alpha_{s+i} - \alpha_s)\mathbf{F}^2\end{aligned}\tag{S1}$$

where  $\mathbf{d}_{s+\text{TS}^*}$  and  $\alpha_{s+\text{TS}^*}$  ( $\mathbf{d}_{s+\text{R}^*}$  and  $\alpha_{s+\text{R}^*}$ ) are the electric dipole moment and polarizability of the whole bounded system consisted of adsorbed transition state (reactant) and the slab used to model the surface;  $\mathbf{d}_{s+i}$  and  $\alpha_{s+i}$  are the electric dipole moment and polarizability of the whole bounded system consisted of adsorbed  $i$  and the slab;  $\mathbf{d}_s$  and  $\alpha_s$  are the electric dipole moment and polarizability of the clean slab. As the surface electric field is perpendicular to the metal surface, only the out-of-plane dipole moment and polarizability are relevant for energetics under EEFs. All parameters needed to compute  $\Delta\Delta E_a[\mathbf{F}]$  and  $\Delta E_{\text{ad}}[\mathbf{F}]$  using the analytical relationships (Equations 2-3 in the main text and Equation S1 here) for elementary reactions of steam reforming of methanol (SRM) are listed in TABLE S1 and S2. Our finite-field DFT modeling shows that the structure of adsorbate such as  $\text{H}_2\text{O}$  is sensitive to the EEF (Fig. S1). The analytical relationships derived within the harmonic approximation remain accurate enough for quantifying the EEF-induced energy change.

---

\* liushi@westlake.edu.cn

TABLE S1.  $\mathbf{d}$  and  $\alpha$  of species on Ni(111) surface

Species	$\mathbf{d}_{s+i} - \mathbf{d}_s$ ( $e\text{\AA}$ )	$\alpha_{s+i} - \alpha_s$
CH <sub>3</sub> OH*	0.36	0.314
CH <sub>3</sub> O*	0.28	0.155
CH <sub>2</sub> O*	0.03	0.102
CHO*	0.03	0.102
CO*	-0.18	0.098
O*	-0.08	0.000
OH*	0.25	0.037
CO <sub>2</sub> *	-0.27	0.241
H <sub>2</sub> O*	0.23	0.347
CH*	0.08	0.045
C*	-0.06	0.004
H*	-0.01	0.000

TABLE S2.  $\mathbf{d}$  and  $\alpha$  of transition states on Ni(111) surface

Reaction	$\mathbf{d}_{s+\text{TS}^*} - \mathbf{d}_s$ ( $e\text{\AA}$ )	$\alpha_{s+\text{TS}^*} - \alpha_s$
CH <sub>3</sub> OH* + * $\longleftrightarrow$ CH <sub>2</sub> O* + H*	0.43	0.32
CH <sub>3</sub> O* + * $\longleftrightarrow$ CH <sub>2</sub> O* + H*	0.22	0.135
CH <sub>2</sub> O* + * $\longleftrightarrow$ CHO* + *	0.05	0.106
CHO* + * $\longleftrightarrow$ CH* + O*	0.03	0.053
CH* + * $\longleftrightarrow$ C* + H*	-0.04	0.016
CO* + O* $\longleftrightarrow$ CO <sub>2</sub> * + *	-0.25	0.151
OH* + * $\longleftrightarrow$ O* + H*	-0.06	0.000
CO <sub>2</sub> * + * $\longleftrightarrow$ CO <sub>2</sub> *	-0.06	0.139

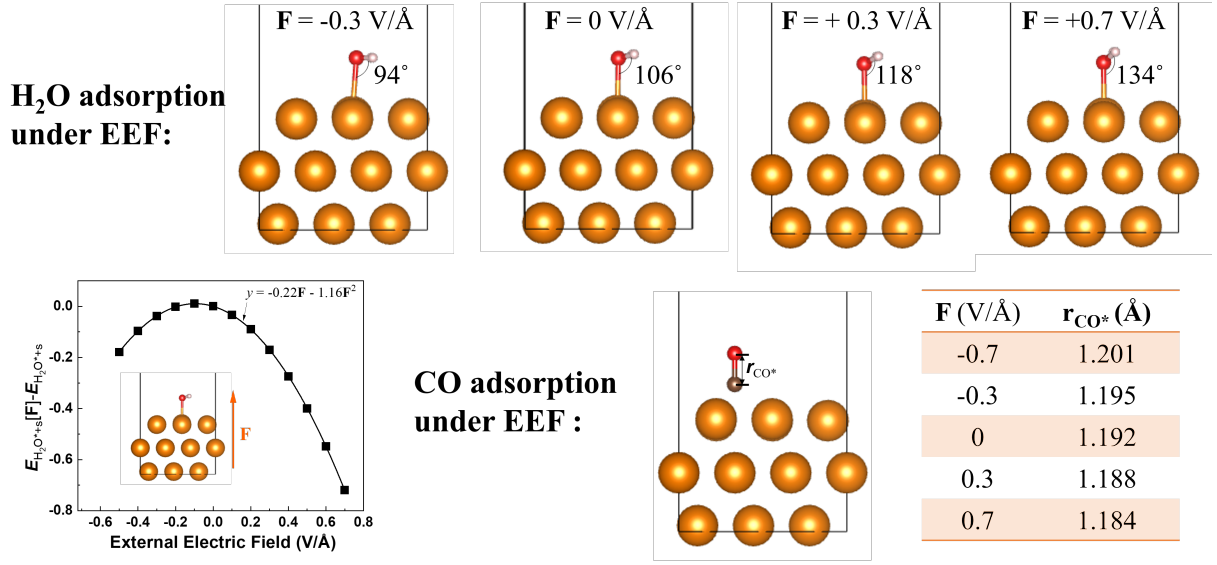


FIG. S1. EEF effect on the structures of H<sub>2</sub>O and CO adsorbed on Ni(111) surface. The EEF-induced energy change can be well described with the harmonic approximation.

## II. MICROKINETICS OF EEF-CATALYZED SRM ON NI(111)

For an elementary reaction, the rate constants  $k$  computed from DFT and transition state theory is fitted to the form of  $k = AT^b \exp(-\frac{\Delta E_a}{RT})$  where  $A$  is a temperature-independent parameter and  $T^b$  describes the temperature dependence of the frequency factor. The EEF-induced change in the activation energy  $\Delta\Delta E_a$  can be expressed as  $\Delta\Delta E_a = -\Delta\mathbf{d} \cdot \mathbf{F} - \frac{1}{2}\Delta\alpha\mathbf{F}^2$ , where  $\Delta\mathbf{d} = \mathbf{d}_{s+\text{TS}^*} - \mathbf{d}_{s+\text{R}^*}$ ,  $\Delta\alpha = \alpha_{s+\text{TS}^*} - \alpha_{s+\text{R}^*}$ . All parameters for the microkinetic modeling of SRM under EEFs are listed in TABLE S3. The results from the microkinetic modeling is compared with experiments (Fig. S2), revealing satisfying agreement. The reaction conditions used are S:M = 3:1, inlet velocity = 10 cc/min, activation surface = 0.14 m<sup>2</sup>.

TABLE S3. Parameters for the microkinetic modeling of SRM under EEFs.  $A$  in the unit of mol/s/cm<sup>2</sup> and  $\Delta E_a^0$  in the unit of kJ/mol. See additional details in Table notes.

$N$	Reaction	$A$	$b$	$\Delta E_a^0$	$\Delta d$ (eÅ)	$\Delta\alpha$
1	$\text{CH}_3\text{OH} + * \rightarrow \text{CH}_3\text{OH}^*$	$5.59 \times 10^{-2}$	-0.5	0.00	0.00	0.00
2	$\text{CH}_3\text{OH}^* \rightarrow \text{CH}_3\text{OH} + *$	$8.13 \times 10^{12}$	-2.06	37.9	0.36	0.16
3	$\text{CH}_3\text{OH}^* + * \rightarrow \text{CH}_3\text{O}^* + \text{H}^*$	$1.13 \times 10^{22}$	-5.71	15.4	-0.07	-0.01
4	$\text{CH}_3\text{O}^* + * \rightarrow \text{CH}_3\text{OH}^* + *$	$1.35 \times 10^{11}$	-1.40	53.50	-0.15	-0.09
5	$\text{CH}_3\text{O} + * \rightarrow \text{CH}_2\text{O}^* + \text{H}^*$	$8.81 \times 10^{16}$	-4.23	86.80	0.06	0.01
6	$\text{CH}_2\text{O} + \text{H}^* \rightarrow \text{CH}_3\text{O}^* + *$	$1.10 \times 10^6$	-0.13	61.00	-0.19	-0.02
7	$\text{CH}_2\text{O} + * \rightarrow \text{CHO}^* + \text{H}^*$	$2.53 \times 10^9$	-1.74	24.30	-0.02	0.00
8	$\text{CHO}^* + \text{H}^* \rightarrow \text{CH}_2\text{O}^* + *$	$8.40 \times 10^3$	0.35	65.90	-0.02	0.00
9	$\text{CHO}^* + * \rightarrow \text{CO}^* + \text{H}^*$	$1.35 \times 10^7$	-0.68	37.3	0.13	-0.02
10	$\text{CO}^* + \text{H}^* \rightarrow \text{CHO}^* + *$	$2.43 \times 10^1$	1.16	146.5	-0.17	-0.02
11	$\text{CHO}^* + * \rightarrow \text{CH}^* + \text{O}^*$	$8.90 \times 10^4$	-0.22	100.41	0.00	0.02
12	$\text{CH}^* + \text{O}^* \rightarrow \text{CHO}^* + *$	$6.18 \times 10^4$	0.00	120.14	-0.03	0.00
13	$\text{CH}^* + * \rightarrow \text{C}^* + \text{H}^*$	$1.38 \times 10^{10}$	-1.47	129.76	0.12	0.01
14	$\text{C}^* + \text{H}^* \rightarrow \text{CH}^* + *$	$5.50 \times 10^6$	-0.40	79.87	-0.02	-0.01
15	$\text{CO}^* + \text{O}^* \rightarrow \text{CO}_2^* + *$	$5.53 \times 10^4$	0.09	134.80	-0.01	-0.03
16	$\text{CO}_2^* + * \rightarrow \text{CO}^* + \text{O}^*$	$5.47 \times 10^1$	0.76	38.20	-0.02	0.05
17	$\text{H}_2\text{O}^* + * \rightarrow \text{OH}^* + \text{H}^*$	$1.6 \times 10^{21}$	-5.73	17.30	0.23	0.16
18	$\text{OH}^* + \text{H}^* \rightarrow \text{H}_2\text{O}^* + *$	$5.16 \times 10^8$	-1.04	60.20	0.25	0.02
19	$\text{OH}^* + * \rightarrow \text{O}^* + \text{H}^*$	$6.40 \times 10^{19}$	-5.06	104.90	0.31	0.02
20	$\text{O}^* + \text{H}^* \rightarrow \text{OH}^* + *$	$5.90 \times 10^9$	-1.43	109.50	0.00	0.00
21	$\text{H}_2 + 2* \rightarrow 2\text{H}^*$	$7.63 \times 10^{-6}$	1.39	5.70	0.00	0.00
22	$2\text{H}^* \rightarrow \text{H}_2 + 2*$	$1.05 \times 10^3$	1.61	86.3	0.00	0.00
23	$\text{H}_2\text{O} + * \rightarrow \text{H}_2\text{O}^*$	$7.48 \times 10^{-2}$	-0.50	0.00	0.00	0.00
24	$\text{H}_2\text{O}^* \rightarrow \text{H}_2\text{O} + *$	$1.50 \times 10^{13}$	-2.46	39.30	0.23	0.16
25	$\text{CO} + * \rightarrow \text{CO}^*$	$6.67 \times 10^{-2}$	-0.50	0.00	0.00	0.00
26	$\text{CO}^* \rightarrow \text{CO} + *$	$2.61 \times 10^{12}$	-1.69	184.30	-0.18	0.05
27	$\text{CO}_2 + * \rightarrow \text{CO}_2^*$	$2.64 \times 10^{-1}$	-0.23	25.34	0.06	-0.07
28	$\text{CO}_2^* \rightarrow \text{CO}_2 + *$	$1.94 \times 10^4$	0.33	20.00	-0.21	0.05

The unit of mol/s/cm<sup>2</sup> can be converted to molecule/s/site by dividing the density of Ni surface sites,  $3.09 \times 10^{-9}$  mol/cm<sup>2</sup>. The unit of frequency factor for a molecular adsorption process (Reaction 1, 21, 23, 25, and 27.) is mol/kPa/s/cm<sup>2</sup>.

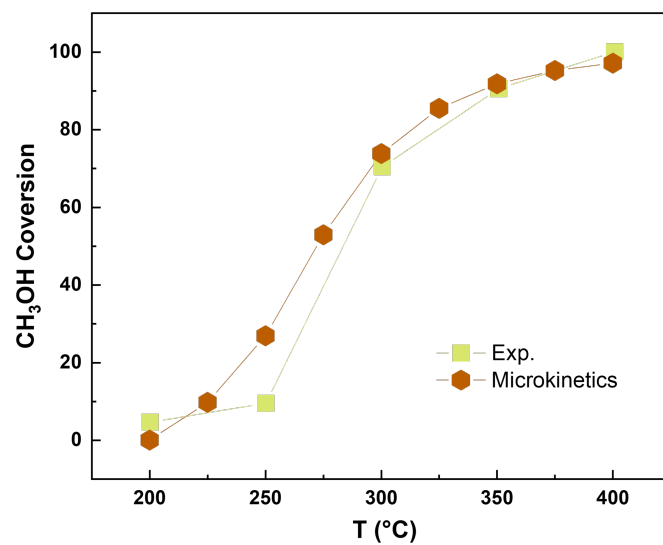


FIG. S2. Comparison of microkinetic modeling and experimental results.

The SRM process includes the water gas shift (WGS) process. Our microkinetic modeling shows that the overall rate of WGS is dictated by the forward rate of  $\text{CO}^* + \text{O}^* \longrightarrow \text{CO}_2^* + ^*$ .

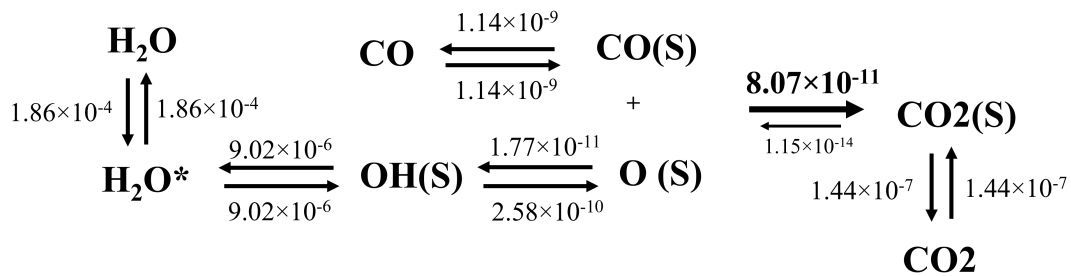


FIG. S3. Reaction flux of WGS at 250°C. The forward rate of  $\text{CO}^* + \text{O}^* \longrightarrow \text{CO}_2^* + *$  is three orders of magnitude faster than its reverse reaction.



#### IV. SIMPLIFIED KINETIC MODEL

The simplified kinetic model of SRM under EEFs consists of six equations:

$$\left\{ \begin{array}{l} \frac{P_{\text{CH}_3\text{OH}}^{\text{in}}}{P_{\text{total}}} \cdot v_{\text{in}} - \frac{P_{\text{CH}_3\text{OH}}^{\text{out}}}{P_{\text{total}}} \cdot v_{\text{out}} = r_{\text{CH}_3\text{OH}} \cdot S \quad (\text{CH}_3\text{OH decomposition}) \\ r_{\text{WGS}}^{\text{out}} \cdot S = P_{\text{CO}_2}^{\text{out}} \cdot v_{\text{out}} \quad (\text{Steady state condition of CO}_2) \\ P_{\text{CH}_3\text{OH}}^{\text{in}} \cdot v_{\text{in}} = (P_{\text{CH}_3\text{OH}}^{\text{out}} + P_{\text{CO}}^{\text{out}} + P_{\text{CO}_2}^{\text{out}}) \cdot v_{\text{out}} \quad (\text{Conservation of C}) \\ (P_{\text{H}_2}^{\text{in}} + P_{\text{H}_2\text{O}}^{\text{in}} + 2P_{\text{CH}_3\text{OH}}^{\text{in}}) \cdot V_{\text{in}} = (P_{\text{H}_2}^{\text{out}} + P_{\text{H}_2\text{O}}^{\text{out}} + 2P_{\text{CH}_3\text{OH}}^{\text{out}}) \cdot v_{\text{out}} \quad (\text{Conservation of H}) \\ (P_{\text{CH}_3\text{OH}}^{\text{in}} + P_{\text{H}_2\text{O}}^{\text{in}}) \cdot v_{\text{in}} = (P_{\text{CH}_3\text{OH}}^{\text{out}} + P_{\text{CO}}^{\text{out}} + P_{\text{H}_2\text{O}}^{\text{out}} + 2P_{\text{CO}_2}^{\text{out}}) \cdot v_{\text{out}} \quad (\text{Conservation of O}) \\ P_{\text{H}_2\text{O}}^{\text{out}} + P_{\text{CO}}^{\text{out}} + P_{\text{CO}_2}^{\text{out}} + P_{\text{H}_2}^{\text{out}} + P_{\text{CH}_3\text{OH}}^{\text{out}} = P_{\text{total}} \quad (\text{Constant pressure condition}) \end{array} \right.$$

$P_x^{\text{out}}$  ( $x = \text{H}_2\text{O}, \text{CO}, \text{CO}_2, \text{H}_2, \text{CH}_3\text{OH}$ ) and  $v_{\text{out}}$  are the partial pressure of gas  $x$  and the total mole velocity of outlet.  $P_x^{\text{in}}$  ( $x = \text{H}_2\text{O}, \text{CO}, \text{CO}_2, \text{H}_2, \text{CH}_3\text{OH}$ ) and  $v_{\text{in}}$  are the partial pressure of gas  $x$  and the total mole velocity of inlet that define the initial condition.  $S$  is the activation surface area.

The rate of  $\text{CH}_3\text{OH}$  decomposition under EEFs ( $r_{\text{CH}_3\text{OH}}[\mathbf{F}]$ ) is

$$r_{\text{CH}_3\text{OH}}[\mathbf{F}] = A_{\text{CH}_3\text{OH}} \cdot \exp\left(-\frac{\Delta E_{a,\text{CH}_3\text{OH}} + \Delta\Delta E_{a,\text{CH}_3\text{OH}}[\mathbf{F}]}{RT}\right) \cdot \frac{P_{\text{CH}_3\text{OH}}}{\sqrt{P_{\text{H}_2}}} \cdot \theta[\mathbf{F}]^2. \quad (\text{S2})$$

Here  $\Delta E_{a,\text{CH}_3\text{OH}} = -51.1$  kJ/mol is the apparent activation energy of  $\text{CH}_3\text{OH}$  decomposition and  $\Delta\Delta E_{a,\text{CH}_3\text{OH}}[\mathbf{F}] = -0.22\mathbf{F} - 0.0675\mathbf{F}^2$  (eV);  $A_{\text{CH}_3\text{OH}} = A_5 \frac{A_1 A_3}{A_2 A_4 \sqrt{A_{21}/A_{22}}} = 5.95 \times 10^{16} T^{-6.87}$  mol/kPa<sup>1/2</sup>/s/cm<sup>2</sup>, where  $A_x$  of reaction  $x$  is taken from TABLE S3;  $\theta[\mathbf{F}]$  is the coverage of active sites. Previous microkinetic modeling showed that  $\text{CO}^*$ ,  $\text{O}^*$  and  $\text{H}^*$  are the main surface species[1]. Therefore, the coverage of active sites under EEFs is,

$$\theta[\mathbf{F}] = \left\{ \begin{array}{l} 1 + A_{\text{CO}^*} P_{\text{CO}} \exp\left(-\frac{E_{\text{ad},\text{CO}^*} + \Delta E_{\text{ad},\text{CO}^*}[\mathbf{F}]}{RT}\right) + A_{\text{O}^*} \frac{P_{\text{H}_2\text{O}}}{P_{\text{H}_2}} \exp\left(-\frac{E_{\text{ad},\text{O}^*} + \Delta E_{\text{ad},\text{O}^*}[\mathbf{F}]}{RT}\right) \\ + A_{\text{H}^*} \sqrt{P_{\text{H}_2}} \exp\left(-\frac{E_{\text{ad},\text{H}^*} + \Delta E_{\text{ad},\text{H}^*}[\mathbf{F}]}{RT}\right) \end{array} \right\}^{-1}$$

Here,  $A_{\text{CO}^*} = \frac{A_{25}}{A_{26}} = 2.56 \times 10^{-14} T^{1.19}$  kPa<sup>-1</sup>,  $A_{\text{O}^*} = \frac{A_{23} A_{17} A_{19}}{A_{24} A_{18} A_{20}} = 2.67 \times 10^{17} T^{-6.46}$ ,  $A_{\text{H}^*} = 8.52 \times 10^{-5} T^{-0.11}$ ,  $E_{\text{ad},\text{CO}^*} = E_{\text{s}+\text{CO}^*} - E_{\text{s}} - E_{\text{CO}^*} = -184$  kJ/mol,  $E_{\text{ad},\text{O}^*} = E_{\text{s}+\text{O}^*} - E_{\text{s}} + E_{\text{H}_2} - E_{\text{H}_2\text{O}} = -5.72$  kJ/mol,  $E_{\text{ad},\text{H}^*} = E_{\text{s}+\text{H}^*} - E_{\text{s}} - 1/2 E_{\text{H}_2} = -40.3$  kJ/mol. The derivations can be found in our previous work [1]. For  $\text{CO}^*$ ,  $\Delta E_{\text{ad},\text{CO}^*}[\mathbf{F}] = 0.18\mathbf{F} - 0.048\mathbf{F}^2$  (eV). We find that the EEF has no effect on the adsorption energy of  $\text{H}^*$  and  $\text{O}^*$ .

Similarity, the rate of WGS based on the reaction pathway in Fig. S3 is,

$$r_{\text{WGS}}[\mathbf{F}] = k_{15}\theta_{\text{CO}*}\theta_{\text{O}*} - k_{16}\theta_{\text{CO}_2*}\theta. \quad (\text{S3})$$

Here,

$$k_{15}\theta_{\text{CO}*}\theta_{\text{O}*} = A_{15}A_{\text{CO}*}A_{\text{O}*}\exp\left(-\frac{\Delta E_{a,+}^{\text{WGS}} + \Delta\Delta E_{a,+}^{\text{WGS}}[\mathbf{F}]}{RT}\right)P_{\text{CO}}\frac{P_{\text{H}_2\text{O}}}{P_{\text{H}_2}}\theta^2$$

$$k_{16}\theta_{\text{CO}_2*}\theta = A_{16}\frac{A_{27}}{A_{28}}\exp\left(-\frac{\Delta E_{a,-}^{\text{WGS}} + \Delta\Delta E_{a,-}^{\text{WGS}}[\mathbf{F}]}{RT}\right)P_{\text{CO}_2}\theta^2$$

$$\Delta\Delta E_{a,+}^{\text{WGS}}[\mathbf{F}] = \Delta\Delta E_{a,-}^{\text{WGS}}[\mathbf{F}] = 0.27\mathbf{F} - 0.1205\mathbf{F}^2$$

$$\Delta E_{a,+}^{\text{WGS}} = E_{\text{TS}^*}^{\text{CO}*+\text{O}* \rightarrow \text{CO}_2*+*} - E_{\text{CO}} - E_{\text{H}_2\text{O}} + E_{\text{H}_2} = -55.22 \text{ kJ/mol}$$

$$\Delta E_{a,-}^{\text{WGS}} = E_{\text{TS}^*}^{\text{CO}*+\text{O}* \rightarrow \text{CO}_2*+*} - E_{\text{CO}_2} = 43.54 \text{ kJ/mol}$$

More detailed derivations can be found in our previous work [1],  $E_{\text{CO}}$ ,  $E_{\text{H}_2\text{O}}$ ,  $E_{\text{H}_2}$  and  $E_{\text{CO}_2}$  are the energies of isolate molecules, respectively.  $E_{\text{TS}^*}^{\text{CO}*+\text{O}* \rightarrow \text{CO}_2*+*}$  is the energy of the transition state of  $\text{CO}* + \text{O}* \rightarrow \text{CO}_2* + *$ . The consistence of simplified kinetics and microkinetics of SRM is shown in Fig. S4. The EEF effects predicted with the simplified kinetic model are consistent with the results of microkinetics (Fig. S5).

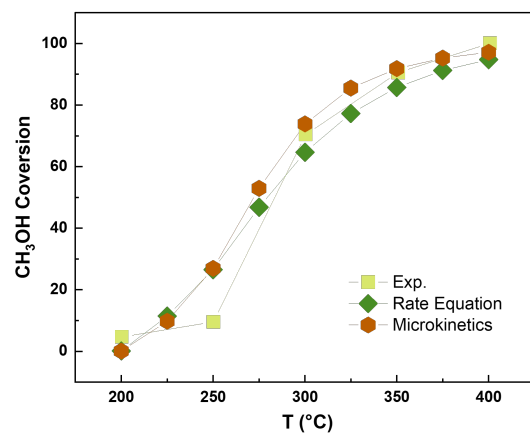


FIG. S4. Comparison between simplified kinetic model with microkinetics and experiments.

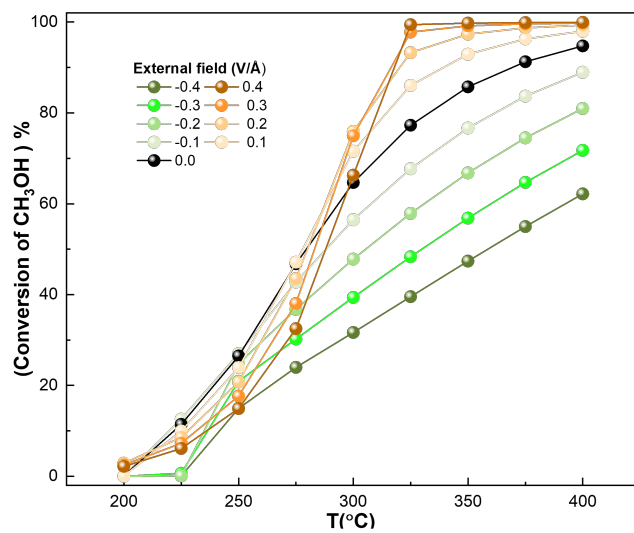


FIG. S5. EEF effects predicted with the simplified kinetic model.

- 
- [1] C. Ke and Z. Lin, Density functional theory based micro- and macro-kinetic studies of nickel-catalyzed methanol steam reforming, *Catalysts* **10**, 349 (2020).